PLANAR TWO-LINK MANIPULATOR CONTROL WITH MULTIPLE-SYNAPSE NEURAL NETWORK CONTROLLER

Benedito Dias Baptista F.(†) and Eduardo Lobo Lustosa Cabral (††)

(†) Instituto de Pesquisas Energéticas e Nucleares – IPEN-CNEN/SP - bdbfilho@net.ipen.br

(††) Escola Politécnica da Universidade de São Paulo, Brazil - elcabral@usp.br

Abstract: **This work presents the position control of a robot manipulator using a new artificial neural network. This neural network is based on a new neuron model with multiple synapses. The synapses' connective strengths are modified through a selective and cumulative process that resembles an unsupervised learning method. These new concepts applied to the position control of the planar two-link manipulator show excellent results.**

***Index terms*— Neural network architecture, Control systems, Manipulator position-control**

I - INTRODUCTION

The purpose of this paper is to present the results of an innovation in the field of artificial neural networks that can be used to control robot arms. The paper consists of six sections. The first section is this introduction. The second section describes the new concepts introduced. The third section shows the application of the neural network in the control of the robot arm. The fourth section presents the results and discussions. The fifth section is a summary of conclusions.

II - THE NEW CONCEPT

The new concepts used in the planar two-link manipulator position control presented in this paper were developed as part of a doctoral thesis conducted between 1994 and 1998, which is described in detail in [1] and [2]. These new concepts are based on biological neuronal circuits and functions and are resumed next:

A. Neuronal Signaling

1) The unit transfer function: The unit transfer function used in this approach is a modified hyperbolic tangent:

$$O = T_N \ tanh\left(\alpha \sum S\right), \tag{1}$$

where O is the output signal, T_N represents the "size" of the unit, α is a gain, and ΣS is the summation of all synaptic input to that unit. The "size" can be set to any convenient values, for instance, to improve the linearity in the range of interest, or to amplify or to reduce the input to output relation.

2) Synaptic transmission modeling: The synaptic transmission process is simulated by a set of Gaussian like functions like that one exemplified in Figure 1 and expressed as:

$$S = \frac{T}{1 + a(I - I_0)^2}, \tag{2}$$

where, T is the "strength" of the synapse, which can be set as any positive value (excitatory) or as any negative value (inhibitory), a is a constant that can be adequately chosen to produce smooth functions according to the number of synapses, I is the signal value that pass through the axon, and, I_0 is the value of I that maximizes S, the output value to the target cell, which is called here "threshold".

Expression (2), that represents a single synaptic terminal, permits amplification and selective response. This function enhances the whole unit transfer function and is much simpler than sigmoidal functions in terms of computation time. With convenient strengths and thresholds, a set of functions like that of equation (2) can produce any kind of continuous function.

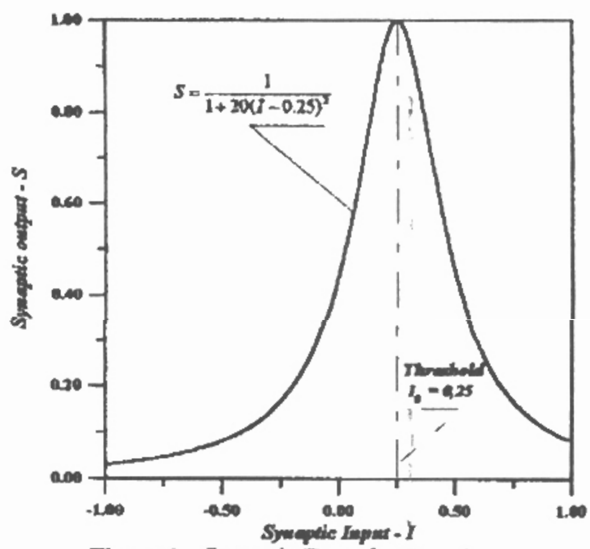

Figure 1 - Synaptic Transfer Function.

B. Learning and Memory Mechanisms

In biological neuronal circuits, a single set of synapses can participate in different forms of learning: *they can be depressed by habituation or enhanced by sensitization.*

More complex forms of learning are *classical conditioning and practice*. The reflexive memory mechanism process suggests the design of a special circuit to implement the learning process. This circuit, shown in Figure 2, scales the error signal via one facilitating inter-unit, that is connected to the output unit synaptic terminals through axo-axonic connections, where the changes are to be effected. The sign of the error dependent signal decides if the process is a presynaptic facilitation or presynaptic inhibition, which will increase or decrease the synaptic strength.

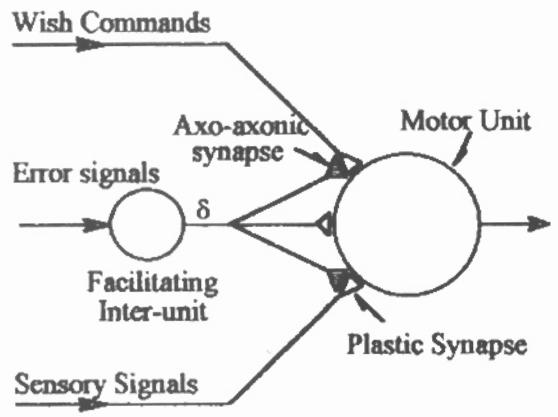

Figure 2 - Synaptic array for the Learning Process.

The change in the synaptic strength due to the learning process is outfitted by a plasticity model, based on memory storage mechanisms. This is done through a cumulative process where the governing term is proportional to the incoming signal (the training signal δ) and its decay rate, as follows:

$$\frac{dC}{dt} = T_c\,\delta - \lambda\, C, \tag{3}$$

where C is the long-term change's trigger factor, δ is the output signal of the facilitating inter-unit, λ is a decay constant, and, T_c is the strength of the facilitating synapse (that controls the rate of change).

According to equation (3) the long-term change's trigger factor (C) can grow in a rate proportional to the learning signal (δ) up to an equilibrium value. This makes the *change in the synapses strength* faster or slower. If the incoming learning signal decreases to zero the long-term change's trigger factor will also decrease to zero, according to the rate established by the decay constant (λ). This means that after a reasonable period of training, when there are no error and no excessive movement, there will be no need for further changes, thus making the process inherently stable.

To complete this idea, an artifice is create to make the changes occurring mainly in the convenient synapses, i.e., in the synapses where the threshold (I_0) is closer to the incoming desired values. This novel characteristic makes the correct synaptic selection, with the strength rate of change of the motor unit synapses (parameter T in equation 2) as a function of the long-term change's trigger factor and of the synaptic threshold. This is implemented by the following expression:

$$\frac{dT_j}{dt} = \frac{C}{1 + a_s(I - I_{0,j})^2}, \tag{4}$$

where T_j is the strength of the *j-th* synapse of the motor unit, a_s is the constant of the Gaussian like function of the facilitating synapse, I is the signal value that comes from the upper control level (the Wish), and, I_0j is the threshold of the synapse.

C. Architectural Design of the Motor Control Unit

The network's main structure concept is represented in Figure 3. It defines a "motor control unit," which summarizes the new concepts applied to control purposes.

In Figure 3 the input pathway from the upper level system ("The Wish" - I_c) and that from the sensory system ("The Actual Condition" - I_s) converge to the unit responsible for sensing the actual error (ε). These signals are linked to the error sense unit with rigid connections that will not change with training. These connections are modeled to make the error unit to sense the actual condition from the sensory system with the opposite sign of the wish signal, i.e., $\varepsilon = I_c - I_s$. This is implemented by equations (5) and (6), bellow.

$$S_{e+} = \frac{1}{N}\left(\frac{2}{1+0.25(I-2)^2}\right) = -S_{i-}; \tag{5}$$

$$S_{e-} = \frac{1}{N}\left(\frac{2}{1+0.25(I+2)^2}\right) = -S_{i+}; \tag{6}$$

where N is the number of redundancies. The schema of multiple branches of synaptic terminals improves the reliability as long as it allows the increase in the number of terminals, what can make a more fail-proof system.

To avoid feeding the network with the rate of change of the sensory signals, an artifice is used to sense these rates within the network. Sensing differences between signals from units in different layers implement this idea. The inter-units responsible for this function are coupled with rigid connections. The output signals of these units in the several levels represent the rates of change of sensory signals. These signals are combined with the error signal in one intermediate unit that makes the connections with the output unit. This signal combination represents the system dynamics as an analogy to the summation of $a_0\varepsilon + a_1 d\varepsilon/dt + a_2 d^2\varepsilon/dt^2 + \ldots$ The coefficient a_0 of the error is implemented by the following synaptic functions that result in a linear transfer function.

$$S_{epe} = \frac{1}{N}\left(\frac{T_e}{1+0.25(I-2)^2}\right); \tag{7}$$

$$S_{ipe} = \frac{1}{N}\left(\frac{-T_e}{1+0.25(I+2)^2}\right); \tag{8}$$

where T_ε is the strength of the error synapse.

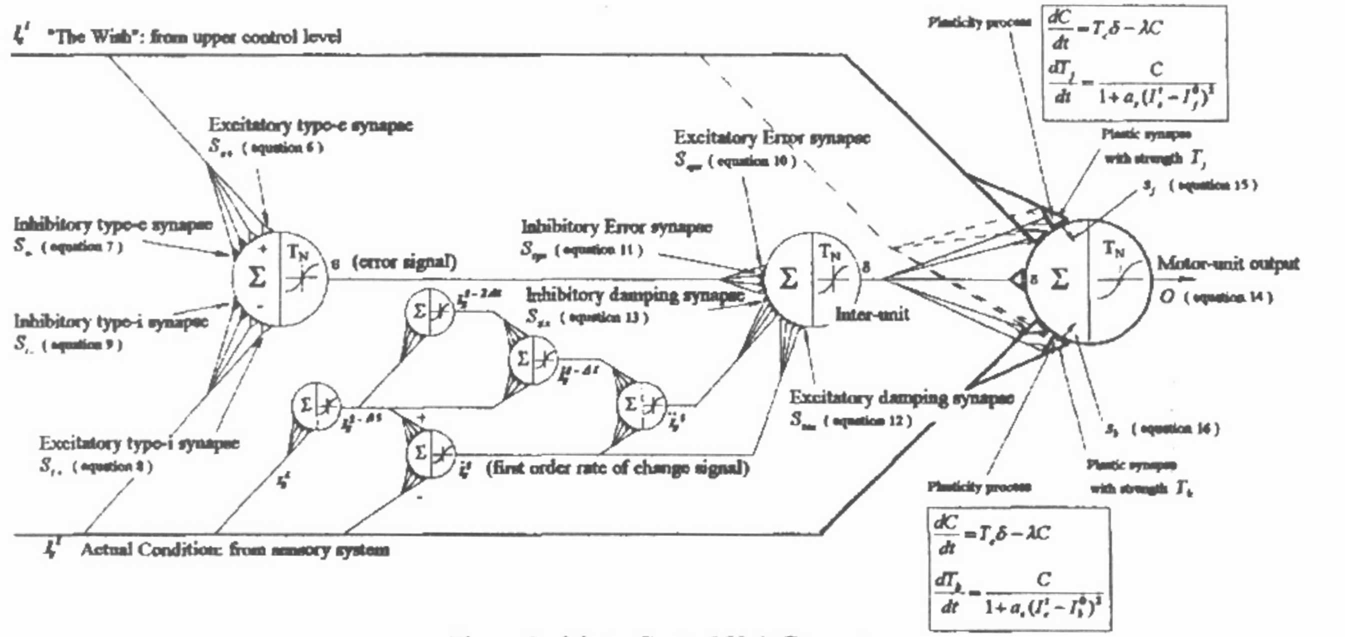

Figure 3 - Motor Control Unit Concept.

The synaptic transfer functions for the connections of the rate of change of the sensory signals with the inter-unit are modeled with damping characteristics of the type of x|x|. This is necessary to attenuate oscillations and to make the process stable even in the presence of high rates of change. Equations (9) and (10) implement the coefficients a_i according to that characteristic. This damping is biologically plausible because we have neurons and muscle cells with damping characteristics.

$$S_{rm} = \frac{1}{N}\left(\frac{T_r}{1+11(I-1)^2}\right); \tag{9}$$

$$S_{rn} = \frac{1}{N}\left(\frac{-T_r}{1+11(I+1)^2}\right); \tag{10}$$

where T_r is the strength of the rate of change synapses.
The sensory and upper level signals are transmitted through two symmetrical (in terms of threshold and strength) sets of synapses, *which are the synapses with plasticity that will be adjusted by learning*. The plastic synapses behavior is represented by:

$$S_j = \frac{T_j}{1+a(I_c - I_{0,j})^2}; \tag{11}$$

$$S_k = \frac{T_k}{1+a(I_s - I_{0,k})^2}; \tag{12}$$

where $T_{j/k}$ is the strength of the *j-th* or of the *k-th* synapse.

Before any training these plastic synapses have no strength, i.e., $T_{j/k} = 0$. The existence of an error signal ε yields a δ signal different from zero that acts to increase or to decrease the long-term trigger factor C given by equation (3). The plastic changes, responsible for the learning process, take place in the motor unit synapses. The wish signal is used to adjust all the plastic synapses even the ones in the actual condition pathway. Detailed description of this motor control unit can be found in references [1] and [2].

III - THE PROBLEM MODELING

The new Motor Control Unit is applied to the position control of a planar two-link manipulator. Simulations of this controller were undertaken to check its performance in terms of control and dexterity learning to reach desired targets.

A. Dynamic Process Modeling

The planar two-link manipulator is a nonlinear, two-degree-of-freedom problem. The variables considered in the manipulator model are shown in Figure 4. The dynamics of this 2-D system is represented by:

$$\tau_1 = H_{11}\ddot{\theta}_1 + H_{12}\ddot{\theta}_2 + h_{122}\dot{\theta}_2^2 + h_{121}\dot{\theta}_1\dot{\theta}_2 + G_1; \tag{13}$$

$$\tau_2 = H_{22}\ddot{\theta}_2 + H_{12}\ddot{\theta}_1 + h_{211}\dot{\theta}_1^2 + G_2; \tag{14}$$

where θ_1 is the angle between the first segment and the x-axis, θ_2 is the angle between the second and first segments, τ_1 and τ_2 are the joint torques 1 and 2 respectively, and the other terms are defines as follows.

$$H_{11} = m_1 l_{c1}^2 + I_1 + [m_2(l_1^2 + l_{c2}^2 + 2l_1 l_{c2}\cos\theta_2) + I_2];$$
$$H_{12} = m_2 l_1 l_{c2}\cos\theta_2 + m_2 l_{c2}^2 + I_2];$$
$$H_{22} = m_2 l_{c2}^2 + I_2;$$
$$h_{122} = -m_2 l_1 l_{c2} sin\theta_2;$$
$$h_{121} = -2m_2 l_1 l_{c2} sin\theta_2;$$
$$h_{211} = m_2 l_1 l_{c2} sin\theta_2;$$
$$G_1 = m_1 g l_{c1}\cos\theta_1 + m_2 g(l_1\cos\theta_1 + l_{c2}\cos(\theta_1 + \theta_2));$$
$$G_2 = m_2 g l_{c2}\cos(\theta_1 + \theta_2).$$

The subscripts 1 and 2 refer to the i-th manipulator segment with mass m_i, total length l_i, distance from the link to the mass center l_{oi} and moment of inertia I_i, and g is the gravitational acceleration.

The dynamics of each electric motor coupled with the manipulator is governed by:

$$J_M \frac{dn}{dt} = \tau_M - \tau - \tau_{PM}, \tag{15}$$

where J_M is the polar moment of inertia of the rotor, n is the rotor speed, τ_M is the motor torque, τ_{PM} is the torque of losses, and τ is the load torque which is given either by equation (13) or (14).

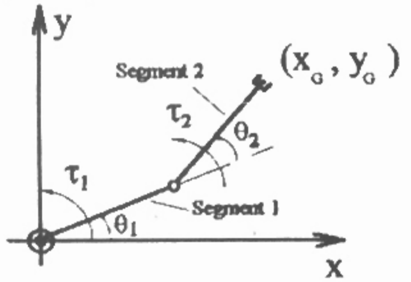

Figure 4 - Two-link Manipulator Model.

The motor torque is expressed as:

$$\tau_M = K_T O, \tag{16}$$

where K_T is the motor/drive torque gain, and O is the output of the attached neural controller.

The torque of losses, τ_{PM}, is composed of two parts: the bearing (τ_{LB}) and the motor losses (τ_{LM}). To describe the bearing losses, static and viscous friction are considered as follows:

$$\tau_{LB} = K_{LB}\mu, \tag{17}$$

where K_{LB} is a constant, proportional to the contact pressure, and μ is the friction factor. This torque can be correlated from data presented in reference [3].

It is assumed that the motor torque of loss is proportional to the square of the motor speed as expressed by:

$$\tau_{LM} = K_{LM}\omega^2, \tag{18}$$

where K_{LM} is a constant function of the motor type.

B. Position Control with the New Neural Network

Since in the manipulator process there are two actuators (the two electric motors) at least two motor control units are necessary. To the purpose of demonstration, the input signals to these control units were restricted to the desired and actual joint angles θ_1 and θ_2. Observe that the joint angular speeds are not necessary because the inter-units sense the rate of change of the joint angles. Also note that in this demonstration the end effector position is treated as a result and not as an objective. This is made to avoid the need of other layers to convert the target end effector position to the desired joint angles.

It is important to say that another system could have been designed, in which each electric motor is controlled by an independent network with all possible combinations of inputs (e.g., θ_1, θ_2, and $\theta_1 + \theta_2$). In this case the two networks should learn which of these inputs are important. But as long as it was decided to design task-specific networks and one can take the profit of its knowledge about the process and how biological systems can deal with it, some simplifications that can improve computer usage are implemented. Considering that the second segment position affects the load on the first segment, the driver of the first motor should be fed with the sum of the outputs of the two controllers. Taking into account that the angle θ_2 is relative to the first segment direction, θ_1 and θ_2 are summed to fed the second controller.

Figure 5 shows the network that represents the two control units coupled with the process. In this figure, sensory pathways are represented by dotted lines, while solid lines represent both upper level signals and intermediate pathways. It can be seen that input inter-units (IN^I) are added to perform the operation of input summations.

Note that in this implementation, the plastic synapses learn only the gravitational torque. Other implementations are possible in such a way that the network learns also the torques generated by the Coriollis and centrifugal forces.

In Figure 5, θ_{1D} and θ_{2D} represent the wish commands (the desired angles), O_1 and O_2 are the output signals from the motor-units that feed the two motor drives, D_1 and D_2, IN^e are the inter-units responsible for sensing the error, IN^{R1} are the inter-units responsible for sensing the first-order rate of change (in this example higher order terms are not needed), IN^F are the learning facilitating inter-units, and IN^D are inter-units used to generate delayed signals, needed to evaluate the rate of change of the signals.

The simulating parameters, training process and performance evaluation of this approach are presented and discussed in the next section.

IV - RESULTS AND DISCUSSION

Table 1 presents the numeric parameters used to simulate the two-link planar manipulator of Figure 5. The main parameters of the neural network components are given in Table 2. The training is performed on-line, i.e., during the performance of some commands of the wish. Changing the wish command according to the numbering sequence of positions presented in Figure 6, performs the unsupervised learning process. A set of 28 target positions is used for training. The manipulator starts from the resting position (-90°), in the stretched configuration, goes clockwise to the -185° position, returns to the resting position, and goes counterclockwise to the +185° position and returns

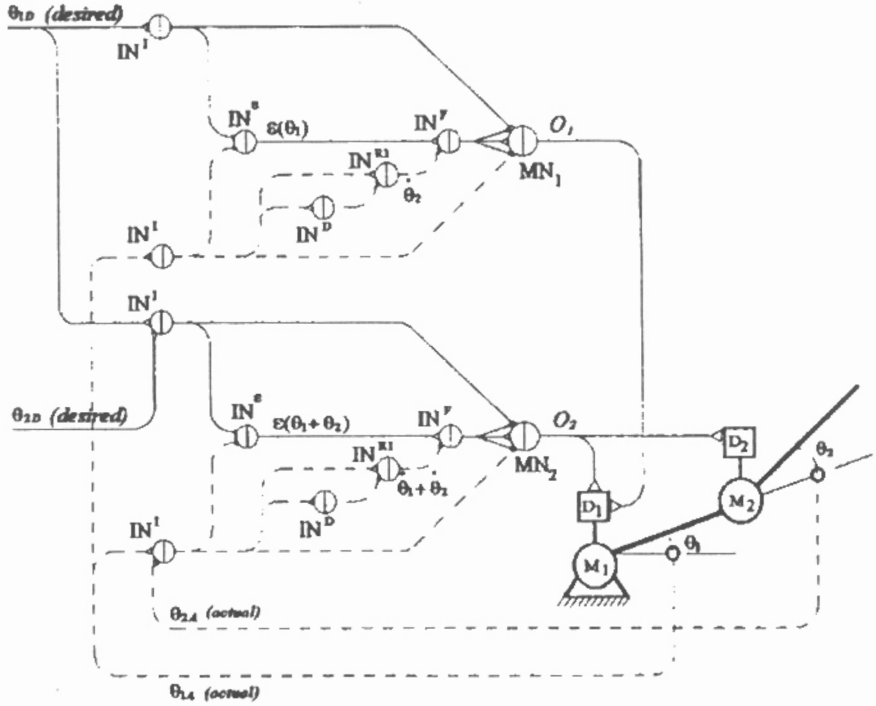

Figure 5 - Simplified outline of the network for the manipulator's control.

again to the resting position. This set of target positions is repeated six times *(six trials)*. The targets pursue duration, t, in each trial are as follows: *first and second trials, t = 5 sec.; third and fourth, t = 10 sec.; and, fifth and sixth, t = 20 sec.*

Table 1 - Parameters for the two-link Manipulator.

Parameter	Segment	
	1	2
Length - L (mm)	707	707
Mass - m (kg)	3.0	2.0
Moment of Inertia - I (kg m^2)	0.041	0.027
Motor Torque Gain - K_T (N M)	60	30
Rotor moment of inertia- J_M (kg m^2)	0.0013	0.0013
Bearing loss constant - K_{LB}	1.0	1.0
Motor loss constant - K_{LM}	25.1	25.1

Table 2 - Parameters for the New Approach Network.

Parameter	Value
Unit's size - T_N (Eq. 1)	2.1
Units gain constant - α (Eq. 1)	0.5
Plastic synapse's constant - a (Eq. 5, 6)	28.8
Number of plastic synapses: sensory to output unit	15
Number of plastic synapses: "wish" to output unit	15
Consecutive thresholds interval ($I_{0,j} - I_{0,j+1}$)	0.1667
Strength of *error synapses* – T_ε (Eqs. 7, 8)	2.5
Strength of *rates synapses* – T_r (Eqs. 9, 10)	0.09
Strength of *facilitating synapses* – Tc (Eq. 3)	0.1
Synaptic strength decay constant - λ (Eq. 3)	10.0
Plastic synapse's *plastic constant* - a_f (Eq. 4)	144.0

After repeating that set of commands six times the system is able to reach all the target positions with reasonable precision and the strengths of the two sets of motor unit synapses, initially zero, grew to that of Figure 7. This "training-phase" last 1960 seconds of simulated time (with only 85 seconds of CPU time in a 166 MHz Pentium Microcomputer). This is much faster than human capabilities and may indicate that the learning process is computationally efficient.

With those synaptic strengths, the next step is to check the response of the network to any kind of input. Thus the plasticity model was blocked (setting $T_c = 0$ in equation 3) to avoid any new strength update in order to observe the generalization capability of the network. Tests are performed over the complete domain of θ_{1D} and θ_{2D} with excellent results. Tests are also performed without blocking the plasticity model, allowing the observation of its stable performance.

Figure 8 exhibits the results of one of these tests, showing the manipulator end effector trajectory to five targets, each one defined by a different wish, which is kept constant during a period of 6 seconds. In this example two positions were also presented in the training set (points 2 and 4) and three positions were not present in the training set (points 3, 5 and 6). The last target is placed in a great distance from the anterior position to observe the network stability with large errors and rates of change. The evolution of the end effector distance from the desired position is presented in Figure 9, which shows the five spikes that represent the transition of the wish commands, which is done in steps. Observe that, even for targets distant more than 2000mm from the current position, the desired position is almost unwavering reached in less than five seconds. In this example the motor units have only 15 synapses per side, with a total of 60 plastic contacts in the two control units. With only 28 "training points" and 70 seconds of training time at each point, the maximum distance error reached during the performance tests is smaller than 5mm.

V - SUMMARY OF CONCLUSIONS

The performance of the novel ANN proposed for the position control of the planar two-link manipulator shows that the option of task-specific networks seems to be a resourcefully way to solve some problems of control.

The use of multiple contacts in each axon terminal increases the integration capability of each unit. Higher classes of connection's transfer functions improve the input-to-output relation, allowing a reduction in the total number of units with expensive sigmoidal functions (synaptic functions are less expensive).

The training task can be performed on-line during the execution of desired commands, *according to an unsupervised learning approach*. The limited training time and the few targets needed to learn, associated with the good results obtained in the task of positioning over an extended domain, show a remarkable ability of this novel ANN for generalization and for controlling the planar two-link manipulator. This new approach implements artificial mechanism resembling habituation or sensitization, provided by facilitating units. The use of a single plasticity model in the synapses enables real time learning while functioning without any physically unexplained mathematical algorithm.

The new ANN is more complex than conventional multilayered back-propagation networks in terms of synaptic arrays and transfer functions but it has the advantage of reducing the total number of units. As the transfer function of the neuron units is more complex than that of the synapses there is a net gain in terms of performance as demonstrated in Section IV. The performance of learning and acting showed in the examples demonstrates that this is certainly a promising concept.

More details, including comparisons with a feed-forward neural network, and the application of this new concept in other applications are presented in references [1] and [2].

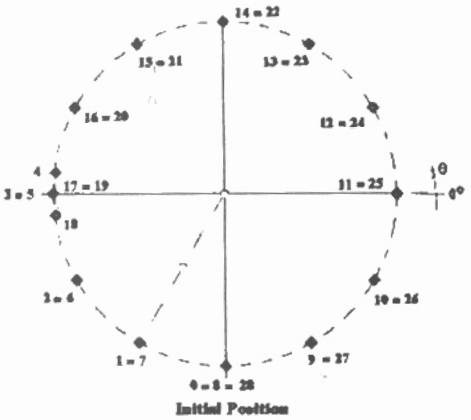

Figure 6 - Training positions set.

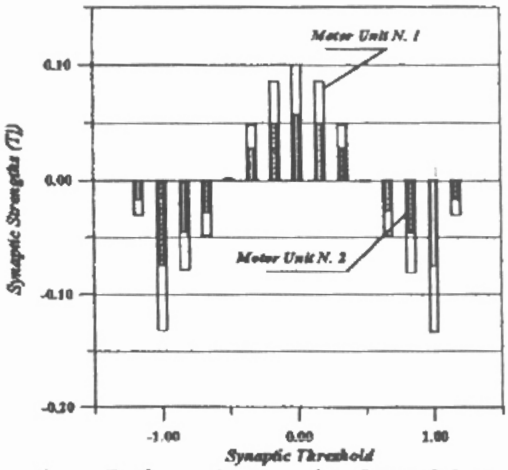

Figure 7 - Synaptic strengths after training.

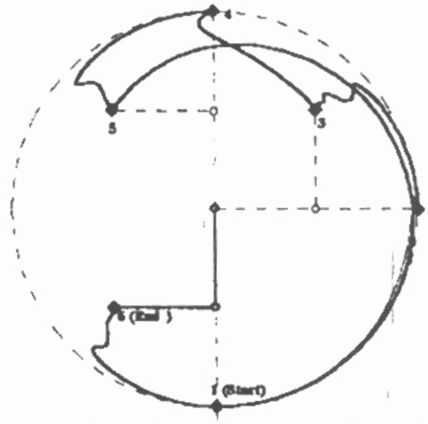

Figure 8 - Manipulator end effector's trajectory.

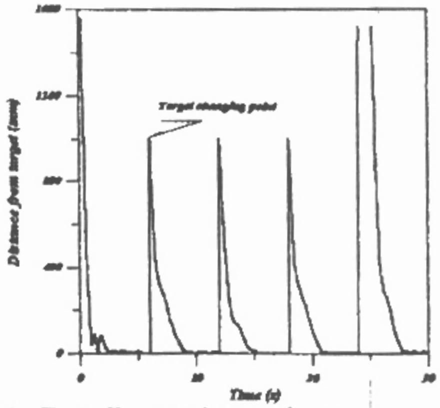

Figure 9 - End effector Distance from Target Position.

Acknowledgment: The authors acknowledge the financial support given by Fundação de Amparo à Pesquisa do Estado de São Paulo (FAPESP) to present this paper.

VI – REFERENCES

[1] Baptista F., B. D., "A New Approach to Artificial Neural Netowrks", *IEEE Transactions on Neural Networks Vol. 9, NO. 6, November* 1998.

[2] Baptista F., B. D., *Redes Neurais para Controle de Sistemas de Reatores*, São Paulo: 1998. Thesis (Doctoral) – Instituto de Pesquisas Energéticas e Nucleares.

[3] Niemann, G., *Maschinenelemente*, Springer-Verlag *OHG*., 1950.